Gelation and Its Effect on the Photophysical Behavior of Poly(9,9-dioctylfluorene-2,7-diyl) in Toluene

Jean-Hong Chen,*,† Chih-Shun Chang,†,§ Ying-Xun Chang,†,§ Chun-Yu Chen,‡,§ Hsin-Lung Chen,*,‡ and Show-An Chen‡

Department of Polymer Materials, Kun Shan University, Tainan Hsien 71003, Taiwan, and Department of Chemical Engineering, National Tsing Hua University, Hsin-Chu 30013, Taiwan

Received October 28, 2008; Revised Manuscript Received December 15, 2008

ABSTRACT: We probed the gelation and its effect on the photophysical property of a conjugated semiconducting polymer, poly(9,9-dioctylfluorene-2,7-diyl) (PF8), in toluene. The conformational structure characterized by the radius of gyration and the persistence length of PF8 in the dilute toluene solution depended strongly on temperature, where the conjugated chains exhibited a more extended conformation as the temperature was raised. The interchain interaction above the overlap concentration induced aggregation of PF8 to form network clusters in the solution. Gelation took place when the semidilute PF8 solutions were cooled and subsequently aged at −20 °C. The gel composed of the dynamically arrested PF8-enriched phase and the isotropic phase due to the occurrence of a macrophase separation at the subambient temperature. The PF8-enriched phase was mesomorphic, consisting of sheetlike aggregates or membranes. A fraction of the PF8 chains or segments within these sheetlike aggregates formed the β-phase which dominated the photoluminescence of the gel. The gel structure could be disrupted by heating to ca. 45 °C, above which the corresponding PL spectra displayed a blue shift because of reduced amount of the β-phase.

Introduction

π-Conjugated polymers constitute a family of organic optoelectronic materials for applications such as light-emitting diodes[1] and photovoltaics.[2] Among a wide variety of conjugated polymers synthesized thus far, polyfluorenes (PFs) have been considered as one of the most important materials[3−5] due to their great potential for uses in blue-light-emitting devices.[6,7]

Poly[9,9-dioctylfluorene-2,7-diyl] (abbreviated as PF8) is a structural archetype of PFs having been extensively studied in the solid state as a model compound for PFs.[8−22] This polymer is crystallizable with the crystal melting point at ca. 170 °C.[23,24] In addition to the stable crystalline α-phase, PF8 exhibits a variety of metastable phases with characteristic photophysical properties depending on the processing condition.[8,9] For example, a mesomorphic β-phase may develop in the polymer films through evaporation of an appropriate solvent[12] or upon the treatment of the polymer films containing one of the other phases by solvent vapor. It was suggested that these treatments induce twists between neighboring monomer units to facilitate a more planar backbone conformation and hence a more extended π-conjugation in the β-phase.[7−9,12−16,18] As a result, this phase displays very narrow line widths in adsorption, prompt and delayed fluorescence, phosphorescence, and photoinduced triplet absorption.[14]

The study of the structure of conjugated polymers in solution state is also very important, since the solution may contain some "precursory structure" that would dominate the structural development in the film-casting process.[8,25,26] The solution structure of conjugated polymers is highly complex. Apart from the effects of the conventional parameters such as solvent quality and concentration, the structure also displays strong time dependence as the dynamics of the system to attain the equilibrium or the metastable equilibrium structure upon the polymer dissolution (assisted by mechanical stirring and heating) is usually very slow. A recent study has demonstrated that even the presence of $\pi-\pi$ complex in the polymer powder used for solution preparation had a great influence on the aggregation behavior of the polymer in solution.[27]

The solution structure of PF8 has also been subjected to a number of studies. For instance, the conformational structure of PF8 in the solution state has been investigated by light scattering.[8] The persistence length (l_{ps}) deduced from the measured radius of gyration with the assumption of wormlike chain model indicated that the polymer chain is semirigid with $l_{ps} \approx 8.5$ nm. Small-angle neutron scattering (SANS) studies revealed that PF8 could be dissolved down to the molecular level in dilute (0.5−1.0 wt %) toluene solutions where they remained as stiff rods.[20] The polymer chains aggregated to form network structure containing domains of aggregates of aligned segments[21] in the semidilute toluene solution.[28] By contrast, the dissolution of PF8 only reached the colloidal level, giving rise to sheetlike aggregates in a poor solvent, methylcyclohexane (MCH).[20] A recent systematic study by Knaapila et al. on the effect of side-chain length on the aggregation of PFs has revealed that the formation of sheetlike aggregate in MCH was rather universal, and the larger length scale structures of these sheets showed an odd−even dependence on the side length.[29] Moreover, PF*n*/MCH ($7 \leq n \leq 9$, n = side chain length) solutions were found to contain the conformational isomer C_β as found for those polymers in the β-phase.

Under appropriate treatments such as increasing polymer concentration and subambient aging, conjugated polymer solutions may undergo physical gelation.[26,30,31] Perahia et al. revealed that the rodlike molecules of poly(2,5-dinonylparaphenylene ethynylene) in toluene solutions aggregated to form large flat clusters driven by the $\pi-\pi$ interaction below ca. 40 °C. When the aggregates were too large to move freely in the solution, a transition into a constrained or jammed phase took place transforming the viscous solution into gel.[26] Chen et al. demonstrated the gelation of poly(2-methoxy-5-(2′-ethylhexyloxy)-1,4-phenylenevinylene) (MEH-PPV)/toluene solution upon prolonged subambient aging. The gelation was found to retard the thermally induced mesophase formation in the subsequently

* To whom correspondence should be addressed. E-mail: kelvench@mail.ksu.edu.tw, hslchen@mx.nthu.edu.tw.
† Kun Shan University.
‡ National Tsing Hua University.
§ The contributions of the three authors to this work are equal.

10.1021/ma802408u CCC: $40.75
Published on Web 01/27/2009

cast films and hence suppressed the red emission at 640 nm for the film cast from the gel.[26]

In a recent study of the phase behavior and solution structure of PFs, Knaapila et al. noted that the PFn ($6 \leq n \leq 9$)/MCH solutions became viscous or gel-like when the solutions were cooled to −25 °C.[31] Their mean-field theoretical model coupled with the small-angle scattering results (showing the existence of sheetlike aggregates in the gels and the structural order−disorder transition from sheetlike structure to fully dissolved rodlike chains upon heating from −25 to 85 °C) had shed light into the driving force of the gelation. A membrane phase in which the PF chains packed to form bilayered sheets was predicted to exist over a narrow temperature range, while the nematic−isotropic coexistence was found to dominate the phase diagram in the phase-separated region. However, although the systems tended to demix upon lowering the temperature, the phase separation occurred very slowly due to the network of the membranes already existed in the solution. Consequently, the formation of the membrane may supersede the lyotropic−isotropic demixing, and the metastable membrane structure was eventually kinetically arrested.

In this study, we demonstrate that physical gelation is also accessible in the solutions of PF8 with toluene, which is a better solvent than MCH, as long as the solutions were aged at sufficiently low temperature (e.g., −20 °C). The gelation process and the thermally induced gel-to-sol transition probed by dynamic light scattering (DLS) and SANS will be presented, and the effect of gelation on the photophysical properties detected by UV−vis and photoluminescence (PL) spectroscopy will be discussed in connection with the development of the β-phase upon gelation. For the clarity of discussion, we will also present the conformational parameters of PF8 in dilute toluene solutions ($c < c^*$; c^* = overlap concentration) at different temperatures deduced from static light scattering (SLS) and also the dynamic behavior of the polymer over a broad concentration range (from $c < c^*$ to $c > c^*$) probed by DLS.

Experimental Section

Preparations of Solutions and Gels. Poly(9,9-dioctylfluorene-2,7-diyl) (PF8) end-capped with dimethyl phthalate was obtained from American Dye Source Inc. The weight-average molecular weight (M_w) was 128 000 g/mol measured by SLS in this work. The solutions of PF8 and toluene were prepared by stirring their mixtures at ca. 40 °C for 12 h, where macroscopically homogeneous solutions were observed by the naked eye. The polymer solutions with concentrations ranging from 0.001 to 3.0 wt % were prepared here. The critical overlap concentration of PF8 in toluene estimated via $c^* \approx M/N_A R_g^3$ was ca. 0.043 wt %. For the dilute solutions ($c < 0.05$ wt %) thus prepared, the solutions were further filtered through 0.45 μm PTFE filters (Millipore) to remove the dust particles prior to the static light scattering (SLS) measurements. The polymer solutions were allowed to equilibrate at room temperature (ca. 25 °C) for 12 h prior to the measurements. The PF8/toluene gels were prepared by aging the solutions with the concentrations of 0.5, 1.0, 2.0, and 3.0 wt % at −20 °C for 24 h.

Light Scattering Measurements. The SLS measurements were carried out using an ALV/CGS-3 light scattering spectrometer equipped with an ALV/LSE-5003 multiple-τ digital correlator. The JDS-Uniphase solid-state He−Ne laser having the output power of ca. 22 mW at the operating wavelength of 632.8 nm was used as the light source. The reciprocal reduced scattering intensity, Kc/R_θ, was obtained, where c is the concentration of polymer and R_θ is the reduced intensity. The optical constant K for vertically polarized light was calculated according to $K = 4\pi^2 n_0^2 (dn/dc)^2/N_A\lambda^4$, where n_0 is the refractive index of the solvent, dn/dc is the refractive index increment with respect to concentration, λ is the wavelength of light in vacuum, N_A is Avogadro's constant, and θ is the scattering angle. The second virial coefficient, A_2, the z-average radius of gyration, R_g, and the weight-average molecular weight, M_w, are related to Kc/R_θ via the well-known Zimm equation, viz.[32]

$$\frac{KC}{R_\theta} = \frac{1}{\bar{M}_w}\left[1 + \frac{16}{3}\pi^2\frac{R_g^{\,2}}{\lambda^2}\sin^2(\theta/2) + ...\right] + 2A_2C + ... \quad (1)$$

The values of the refractive index increment, dn/dc, for the PF8 in toluene solutions at 20 and 50 °C were 8.47×10^{-4} and 8.32×10^{-4} mL g^{-1}, respectively, as measured by an Optilab DSP differential refractometer (Wyatt Tech. Co.) with the laser wavelength of 632.8 nm.

DLS was utilized to probe the gelation process and the thermally induced gel-to-sol transition. By this technique, the increase of hydrodynamic volume in the gelation region may be monitored, and the identification of the sol−gel transition is feasible.[33] The profile of the normalized correlation function changes with increasing concentration of associating macromolecules from stretched exponential function to a power law at the gel point and dynamics of the gelation slows down as the gel point is approached.[33−36] In this study, the DLS experiments were performed using ALV light scattering spectrometer with an ALV/LSE-5003 multiple-τ digital correlator over the time range $10^{-8}-10^3$ s. The autocorrelation function of the light scattering intensity, $G(q,t) = \langle I(q,t)I(q,0)\rangle/\langle I(q,0)^2\rangle$, with $I(q,0)$ the mean light scattering intensity at a scattering vector q was measured at different scattering angles, θ. DLS is a highly effective tool for probing the dynamic behavior of polymer chains, on different length and time scales, in solution state. When the polymer chain obeys Gaussian statistics, the measured normalized intensity correlation function $g^2(t)$ is related to the normalized electric correlation function $g^1(t)$ through the Siegert relation.[37,38]

$$g^{(2)}(\tau) = 1 + \beta|g^{(1)}(\tau)|^2 \quad (2)$$

For a system exhibiting a distribution of collective motions, $g^{(1)}(\tau)$ can be represented by the superposition of exponential decay functions. Laplace inversion routine of $g^{(1)}(\tau)$ was performed to yield the distribution of relaxation times $A(\tau)$, viz.

$$g^{(1)}(\tau) = \int_0^\infty A(\tau)\exp(-t/\tau)\,d\tau \quad (3)$$

The translational diffusion coefficient distribution was obtained from $A(\tau)$, and the hydrodynamic radius distribution was eventually obtained using the Stokes−Einstein equation, $R_h = k_B T/(6\pi\eta D)$, where k_B is the Boltzmann constant, T is absolute temperature, D is the diffusion coefficient, and η is solvent viscosity.

Small-Angle Neutron Scattering (SANS) Experiments. SANS experiments over a scattering vector ($q \equiv 4\pi\sin(\theta/2)/\lambda$ where θ is the scattering angle and λ the wavelength) range of ca. 0.004−0.4 Å^{-1} were carried out using the 30 m SANS instrument at the Center for Neutron Research, National Institute of Standards and Technology. The incident neutron beam was 0.8 nm in wavelength, with resolution $\Delta\lambda/\lambda = 0.15$. The scattering intensity was corrected for background and parasitic scattering, placed on an absolute level using a calibrated secondary standard, and circularly averaged to yield the scattering intensity $I(q)$. The incoherent background from the pure solvent was measured, corrected for the volume fraction of PF8, and subtracted from the reduced SANS data.

Spectral Characterizations. The UV−vis absorption measurements for the $\pi-\pi^*$ and β-phase absorption of PF8 were performed using a Hitachi U-3010 spectrophotometer. The quartz cells of 10 mm thickness were used to measure the spectra of the dilute solutions, while for the semidilute viscous solutions and gels, the samples were sandwiched between two microscope cover glasses to obtain the solution or gel layers of about 100 μm in thickness. The reported absorbances of the samples have been corrected for the solvent background.

The PL spectra were recorded by using a Perkin-Elmer LS55 spectrophotometer. The samples were placed in sealed glass tubes with the thickness of 1 cm for the measurements. The excitation

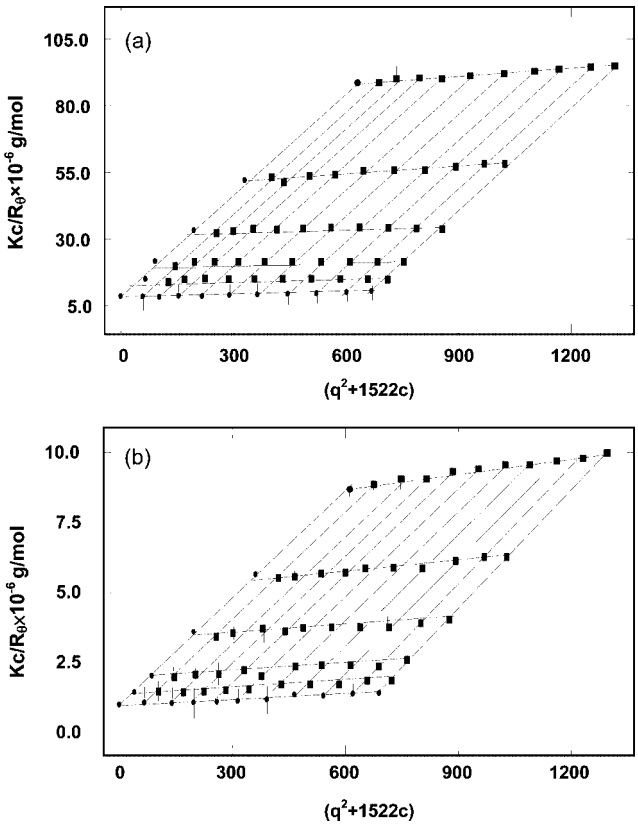

Figure 1. Zimm plots of PF8/toluene dilute solutions at (a) 25 ± 0.1 °C and (b) 50 ± 0.1 °C.

Table 1. Conformational Parameters of PF8 in Dilute Toluene Solution Obtained from the Static Light Scattering Experiments at 25 and 50 °C

	A_2 (mol dm^3 g^{-2})	R_g (nm)	L (nm)	l_{ps} (nm)
25 °C	0.165	24.9	190.3	9.8
50 °C	2.093	46.1	190.3	33.5

wavelength was 320 nm. The temperature-dependent experiments were realized by using a thermostat tube heating system.

Results and Discussion

For the clarity of discussion, we will also present the background information concerning PF8/toluene solution, which includes the temperature-dependent conformational structure of the polymer in dilute solution and the dynamic behavior of the solutions over a broad concentration range probed by DLS.

Conformational Structure of PF8 in Dilute Toluene Solution. In this study, the conformational structures of PF8 in dilute toluene solutions ($c < c^*$) at two temperatures, 25 and 50 °C, were probed by SLS at the concentration range between 0.001 and 0.05 wt %. The estimated c^* of PF8 under study was 0.043 wt %. The previous studies of the solution structure of PF8 indicated that the polymer chains remained well dispersed in the toluene solution,[29] while significant interchain aggregation took place only above certain concentration (ca. 1 wt %).[28] Consequently, we considered the SLS data of the dilute toluene solutions to be contributed predominantly by the molecularly dissolved PF8 chains in the solvent.

Figure 1 shows the Zimm plots of PF8/toluene dilute solutions at the two temperatures. The values of A_2 and R_g obtained through the extrapolation to zero concentration and zero angle, respectively, are listed in Table 1. It can be seen that both A_2 and R_g increased significantly as the temperature was raised from 25 to 50 °C, namely, from the values of 0.165 mol dm^3 g^{-2} and 24.9 nm to the values of 2.093 mol dm^3 g^{-2} and 46.1 nm. This observation attested that the attractive interaction between PF8 and toluene became stronger at higher temperature so as to induce a greater extension of the PF8 chains. Fytas et al. indicated that the conformation of a PF bearing a branched side chain, poly(9,9-bis(2-ethylhexyl)fluorene-2,7-diyl) (PF2/6), in dilute toluene solution could be described by the wormlike chain with the persistence length of l_{ps}= 7 ± 0.5 nm at 20 °C.[39] However, a recent SANS study by Knaapila et al. has revealed that PF2/6 and PF8 chains were essentially rodlike in toluene solutions. The difference may stem from the different working concentration regimes for these two scattering techniques. The solution concentration for SLS measurement is typically very low ($c < c^*$), while for SANS experiment the working concentration is usually much higher (usually well above c^* for conjugated polymer solution) to obtain the intensity data with reasonably good signal-to-noise ratio. The persistence length of conjugated hairy-rod polymers has been found to increase obviously with increasing concentration.[30,40] The concentration dependence of chain rigidity may be attributed to the excluded volume interaction between the rigid segments constituting the polymer chains, which is analogous to the excluded volume interaction between rodlike molecules that leads to the formation of nematic phase in the solution state. At higher concentration the excluded volume interaction between the rodlike segments became more significant; in this case, the polymer chains stretched more to reduce this interaction so as to increase their persistence length. Consequently, a conjugated polymer chain may display wormlike conformation with l_{ps} being smaller than its contour length in the dilute solution, while the chain extends like a rod in the semidilute regime due to prevalent interchain interaction.

Here we approximate the conformation of PF8 in dilute toluene solution by the wormlike chain model. In this case, the radius of gyration is given by the Kratky−Porod equation[41]

$$R_g^2 = \frac{l_{ps}L}{3} = \frac{l_{ps}l_0M}{3M_0} \quad (4)$$

where L is the contour length, M_0 is the monomer molecular weight, l_0 is the monomer length, and M is the molecular weight of the polymer. The molecular weight of PF8 obtained from the SLS data at 25 ± 0.1 °C was ca. 128 000 g mol^{-1}, and the monomer molecular weight and length were 388 g mol^{-1} and 0.75 nm,[8] respectively. The contour length of the PF8 chain was thus ca. 190.3 nm, and the persistence lengths calculated from eq 4 were 9.8 and 33.5 nm at 25 and 50 °C, respectively, which again verified the promotion of the stiffness of PF8 chain in toluene dilute solution with increasing temperature.

Dynamic Behavior of PF8/Toluene Solution and Gel Probed by DLS. DLS was employed here to probe the dynamic behavior of PF8 in toluene solutions with a broad concentration range (i.e., from $c < c^*$ to $c > c^*$), from which the dispersion state of the polymer was elucidated. In the dilute regime where the interaction between the polymer chains is insignificant, DLS probes the translational motion of the individual chains; as such, the correlation length corresponds to the average hydrodynamic radius of the polymer chains. In the semidilute regime, the relaxation rate of the polymer is slowed down because the mobility of the chain segments is constrained by each other.[42,43] An even slower relaxation mode associated with the motion of the clusters can be identified when the polymer chains undergo aggregation in the solution.

Figure 2 shows the normalized intensity correlation function, $g^2(t) - 1$, and the corresponding hydrodynamic radius distribution, R_h (inset), of PF8 in toluene solutions as a function of concentration at 25 °C. With the increase of concentration, the

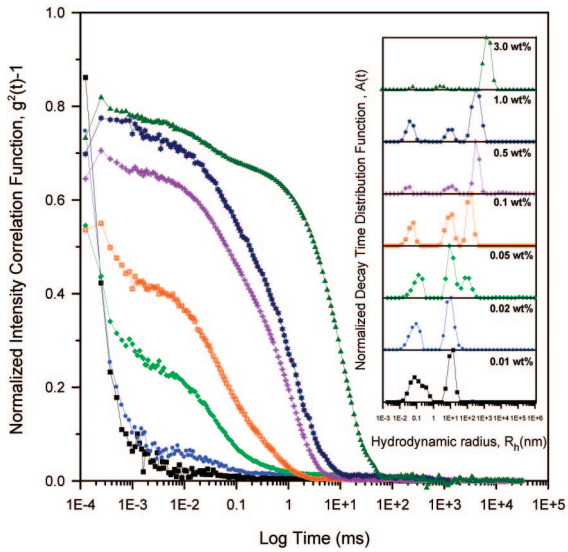

Figure 2. Normalized intensity correlation function, $g^2(t) - 1$, and the hydrodynamic radius (R_h) distribution (inset) of PF8/toluene solutions as a function of concentration at 25 °C (measured at the scattering angle $\theta = 90°$). The R_h spectrum displays up to three relaxation modes. The fast mode with the average R_h of about 0.1 nm represents the motion of the flexible side chains, while the intermediate and the slow mode are attributed to the translational diffusion of individual PF8 chains and the network aggregates formed at concentration above c^*, respectively.

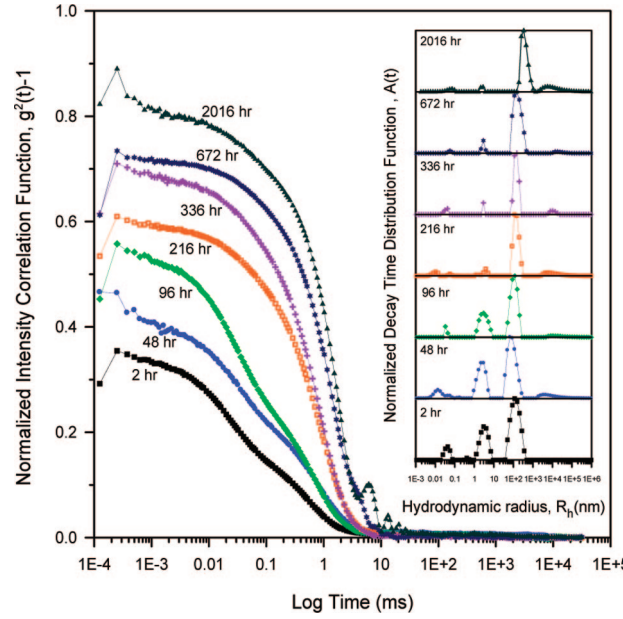

Figure 3. Normalized intensity correlation function, $g^2(t) - 1$, and the hydrodynamic radius (R_h) distribution (inset) of 1.0 wt % PF8/toluene solution as a function of aging time at 25 °C (measured at the scattering angle $\theta = 90°$). The "slowest mode" with the average R_h of ca. 10 μm is found to develop upon aging for more than 48 h.

correlation function was found to shift to longer time along the relaxation time axis. Both the correlation function and the R_h distribution in the dilute regime ($c < 0.02$ wt %) displayed the bimodal mode, where the fast mode with the average R_h of ca. 0.1 nm was associated with the motion of the flexible side chains, while the intermediate mode with the average R_h of about 12 nm was attributed to the translational diffusion of individual PF8 chains. It is noted that in this concentration regime the characteristic hydrodynamic radii did not change with increasing concentration, indicating that the interchain interaction or aggregation was insignificant. In this case, the dimensionless parameter $\rho = R_g/R_h$ can serve as an index for the stiffness of the polymer; generally, ρ is 1.5 for flexible coils, and a larger ρ value indicates a more extended conformation in dilute solution.[38,44] The value of ρ for PF8 in dilute toluene solution was ca. 2.1, which implied that the polymer exhibited an extended conformation in the dilute solution.

The intensity correlation function changed markedly with concentration in the semidilute regime ($c \geq 0.05$ wt %). Here the correlation function grew in intensity and shifted to longer time with the increase of polymer concentration. Moreover, an additional relaxation mode with the average R_h ranging from ca. 100 nm to 1 μm was observed in the R_h spectra. This slow mode even dominated the R_h spectrum above 0.1 wt %. Our previous SANS and NMR study of PF8/toluene solutions had revealed that the polymer was able to aggregate to form network clusters in the semidilute regime;[28] therefore, the observed slow mode was considered to be contributed by the network aggregates of PF8. The development of the aggregates increased the optical heterogeneity, thereby resulting in an increase of light scattering intensity (and hence the intensity correlation function). It is noted that the aggregation of PF8 identified from the presence of a low-q intensity upturn in the SANS profile was found to take place above 1.0 wt %;[28] however, the slow mode detected by DLS already existed at the concentration as low as 0.05 wt % (Figure 2). This means that DLS is a more sensitive probe for the aggregation of PF8 than SANS. It is further noted that the values of the hydrodynamic radii of the fast and the intermediate mode in the semidilute regime were close to those found for the dilute solutions; this implied that a fraction of the PF8 chains remained well dissolved in the solution. When the concentration was lower than 1 wt %, these well-dissolved chains dominated the SANS profiles such that the low-q intensity upturn associated with the network aggregates was hardly identified.

The DLS results have revealed that PF8 chains aggregated in the toluene solution when the overall polymer concentration reached the semidilute regime. It is known that the aggregate structure of conjugated polymers in solution may change upon prolonged isothermal aging due to very slow dynamics associated with the structural reorganization.[26] To demonstrate such a structural reorganization, we conducted an aging-time-dependent DLS experiment for the 1 wt % toluene solutions. In this experiment, the freshly prepared solution (prepared at 80 °C) was cooled to 25 °C and subsequently aged at this temperature for different time periods. The DLS measurement was conducted right after each aging time. Figure 3presents the normalized intensity correlation function and the R_h distribution obtained for different aging times. It can be seen that the intensity of the correlation function grew with the increase of aging time. The average R_h associated with the slow mode also increased with aging time. A new relaxation mode with the average R_h of ca. 10 μm was found to develop upon aging for more than 48 h. This mode was denoted as the "slowest mode". Interestingly, the development of this relaxation mode was found to proceed in expense of the fast and the intermediate mode. This signaled that upon the aging the originally well-dissolved PF8 chains aggregated to form a new entity in which the chain motion was much more constrained than those forming the network clusters (contributing to the slow mode). We postulated that this new entity was the sheetlike aggregate or membrane previously found by Knaapila et al.[20,29,31] Unfortunately, the existence of these aggregates could not be verified from SANS or SAXS for the present case because of their low population in the 1 wt % aged solution.

The development of the slowest mode was greatly accelerated when the aging temperature was significantly lowered to −20 °C. In this case, the originally viscous solution transformed into

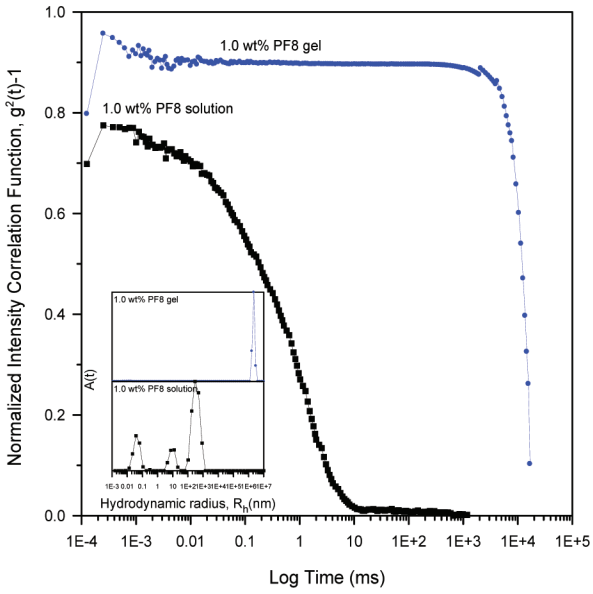

Figure 4. Normalized intensity correlation function, $g^2(t) - 1$, and the hydrodynamic radius (R_h) distribution (inset) of 1.0 wt % PF8/toluene solution and gel. The gel was formed by aging the solution at −20 °C for 24 h.

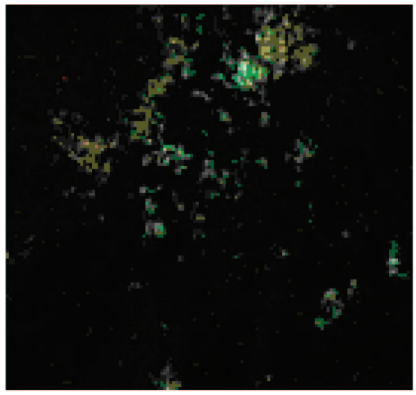

Figure 5. Polarized optical micrograph of the PF8/toluene gel formed by aging the 3 wt % solution at −20 °C for 24 h. The micrograph shows the coexistence of the birefringent regions and dark regions; the former should correspond to the PF8-enriched phase in which the polymer formed a mesophase, and the latter was the isotropic solvent-rich phase.

a gel after 24 h of aging, and the corresponding R_h spectrum displayed only one single mode, i.e., the slowest mode (cf. Figure 4 for the 1 wt % solution and gel). The gelation via subambient aging became even easier for the toluene solutions with higher concentration. The gels thus obtained were visually opaque, which implied the occurrence of phase separation and/or the formation of a mesomorphic phase. Figure 5 displays the polarized optical micrograph of the gel formed from the 3 wt % solution. The micrograph showed the coexistence of the birefringent regions and dark regions; the former should correspond to the PF8-enriched phase in which the polymer formed a mesophase and the later was the isotropic solvent-rich phase. Figure 6 compares the SANS profile of the 3 wt % freshly prepared solution with that of the corresponding gel. In parallel with the study of Knaapila et al.,[31] the SANS intensity of the solution exhibited q^{-1} dependence associated with the form factor of the molecularly dissolved rodlike PF8 chains; the scattering intensity grew significantly, and its q dependence transformed into q^{-2} power law for the gel, which signified the formation of sheetlike aggregates or membrane phase. On basis of the results, we proposed that the gelation of PF8/toluene

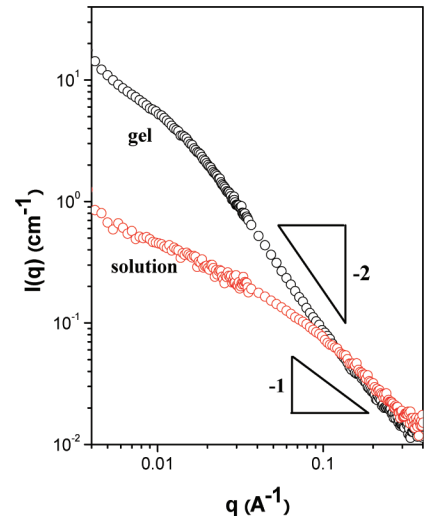

Figure 6. SANS profiles of 3 wt % PF8/toluene solution and gel. The intensity of the solution exhibits q^{-1} dependence associated with the form factor of the molecularly dissolved rodlike PF8 chains. The scattering intensity grows significantly, and its q dependence transforms into q^{-2} power law for the gel, which signifies the formation of sheetlike aggregates.

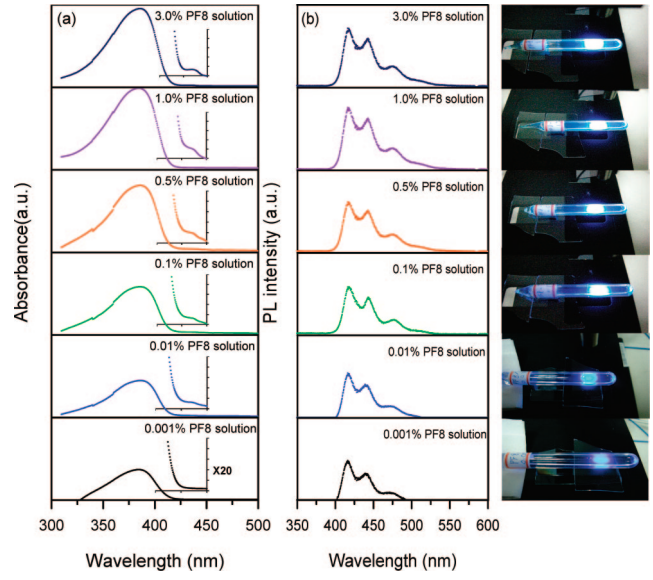

Figure 7. (a) UV−vis and (b) PL spectra of PF8/toluene solutions as a function of concentration. The photographs showing the colors of the light emitted from the solutions are displayed in (c). The inset in (a) shows the expanded view of the tail region of the absorption spectra. It can be observed from (a) that the semidilute solutions display a weak absorption peak/shoulder at 437 nm associated with the PF8 β-phase.

semidilute solution was driven by a macrophase separation at the subambient temperatures, as predicted by the theoretical work of Knaapila et al.[31] In the course of the phase separation, the regions enriched with PF8 gradually developed a mesophase once the polymer concentration exceeded the threshold value for liquid crystal formation. The morphological entity of the liquid crystals thus formed was sheetlike. The presence of the sheetlike aggregates effectively immobilized the PF8-enriched phase, thereby preventing the system from attaining the equilibrium phase-separated morphology by the coarsening process. As a result, the phase-separated structure with extensive connectivity of the PF8-enriched domains (formed at the intermediate stage of the phase separation) was dynamically arrested such that the system attainted the gel property.

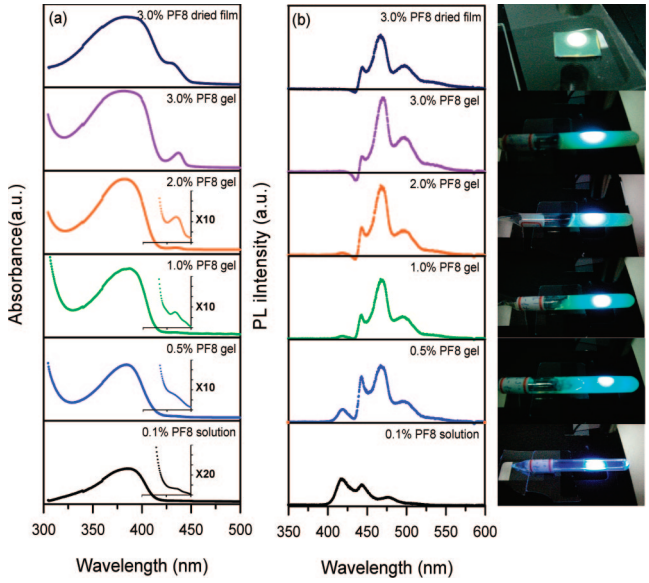

Figure 8. (a) UV−vis and (b) PL spectra of PF8/toluene gels as a function of concentration. The photographs showing the colors of the light emitted from the samples are displayed in (c). The inset in (a) shows the expanded view of the tail region of the absorption spectra. The spectra of the film cast from 3 wt % gel are also shown for comparison. The optical spectra of the film display essentially the same features as the gel.

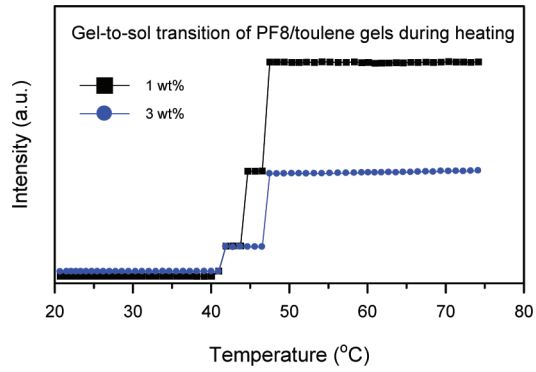

Figure 9. Scattering intensity (measured at the scattering angle of 90° by DLS) of the PF8/toluene gels (formed from 1 and 3 wt % solution) as a function of temperature in a heating cycle. The intensities undergo an abrupt rise at ca. 45 °C, which corresponds to the gel-to-sol transition temperature.

Optical Spectra of PF8/Toluene Solution and Gel. The POM micrograph shown in Figure 5 demonstrated the presence of mesophase in the gel. A possible mesomorphic structure of PF8 is the β-phase, which is a solid-state manifestation of the single isomer C_β with a torsional angle between 160° and 165°.[31] The β-phase can be resolved conveniently from UV−vis or PL spectra as it exhibits narrow line width in its characteristic optical spectra.[7,18,29,45,46] Consequently, these spectroscopic techniques were employed to reveal if the mesomorphic structure observed in the gel was associated with the formation of the β-phase. Figure 7 shows the UV−vis and PL spectra collected at 25 °C of PF8/toluene solutions after subjecting to 48 h of aging at 25 °C. The photographs showing the colors of the light emitted from the solutions are also displayed in Figure 7c. The inset in Figure 7a shows the expanded view of the tail region of the absorption spectra. It can be observed from the absorption spectra that the semidilute solutions displayed a weak absorption peak/shoulder at 437 nm associated with the PF8 β-phase,[7,45] whereas such an absorption signal was absent for the dilute 0.001 wt % solution.

The corresponding PL spectra in Figure 7b showed a weak dependence on concentration, where all solutions displayed emission peaks at 420, 442, and 472 nm associated with the 0−0, 0−1, and 0−2 singlet transition with a shorter illuminophore, respectively.[47] In this case, the individual PF8 chains in the solution could be considered to constitute of various quasi-localized photoemissions or illuminophores.[48−50] At $c \geq 0.1$ wt % a small shoulder located at 500 nm associated with the emission from the longer illuminophores was observed. As revealed by the foregoing DLS results, PF8 could aggregate to form network clusters in the semidilute toluene solutions; therefore, this emission might stem from such an aggregation. Over the concentration range studied, the characteristic emission from the β-phase was not discernible, which may be due to its low population as shown by the corresponding UV−vis spectra.

Figure 8 presents the UV−vis and PL spectra of the PF8/toluene gels formed by aging the corresponding solutions at −20 °C for 24 h. These spectra were clearly different from those of the solutions shown in Figure 7. The gels exhibited a clearer peak/shoulder at 437 nm associated with the β-phase in the absorption spectra. The intensity of this peak grew with increasing polymer concentration in the gel, showing a larger population of the β-phase at higher concentration. In contrast to the solutions, the characteristic emissions of the β-phase became detectable in the PL spectra of the gels, as demonstrated in Figure 8b. Here the emission spectra consisted of two energy regimes: the peak at 420 nm in the higher-energy regime was attributable to the emission from the well-dissolved PF8 chains in the isotropic phase, while the peaks at 440, 470, and 490 nm in the lower-energy regime were associated with the β-phase emission.[12] This observation implied a suppression of the energy transfer from the higher-energy regime (short illuminophores for the individual PF8 chains in the isotropic phase) to the lower-energy one (the β-phase domains in the PF8-enriched phase).

Additionally, we also found that the optical spectra of the film cast from the 3 wt % gel showed essentially the same features as the gel, as seen from Figure 8. This means that the structure in the gel was effectively transferred into the film upon solvent removal. The dominance of the β-phase emission in the gel caused an obvious change of the emission color from blue (for the solution) to green-blue, as shown by the photographs of the samples in Figure 8c.

The spectral characterizations have suggested that the gelation was accompanied by the formation of the β-phase. Coupled with the results of optical microscopy and scatterings, the hierarchical structure of the PF8/toluene gel was proposed as follows. The gel composed of the PF8-enriched phase and the isotropic phase with micrometer in length scale due to the macrophase separation at the subambient temperatures (as revealed by optical microscopy). The PF8-enriched phase was mesomorphic, consisting of the sheetlike aggregates in the nanometer length scale (as revealed by SANS). A fraction of the PF8 chains/segments forming these sheetlike aggregates adopted the β-phase conformation, which dominated the photoluminescence of the gels (as evidenced from the optical spectra).

Thermally-Induced Gel-to-Sol Transition. The PF8/toluene gel may indeed be disrupted by moderate heating; therefore, a gel-to-sol transition was expected to take place by increasing the temperature. Figure 9 presents the scattering intensity (measured at the scattering angle of 90° by DLS) of the PF8/toluene gels (formed from 1 and 3 wt % solution) as a function of temperature in a heating cycle. The intensity was proportional to the population of the well-dissolved PF8 chains in the system because of large scattering angle. It can be seen that the scattering intensity underwent an abrupt rise at ca. 45 °C, which corresponded to the gel-to-sol transition temperature.

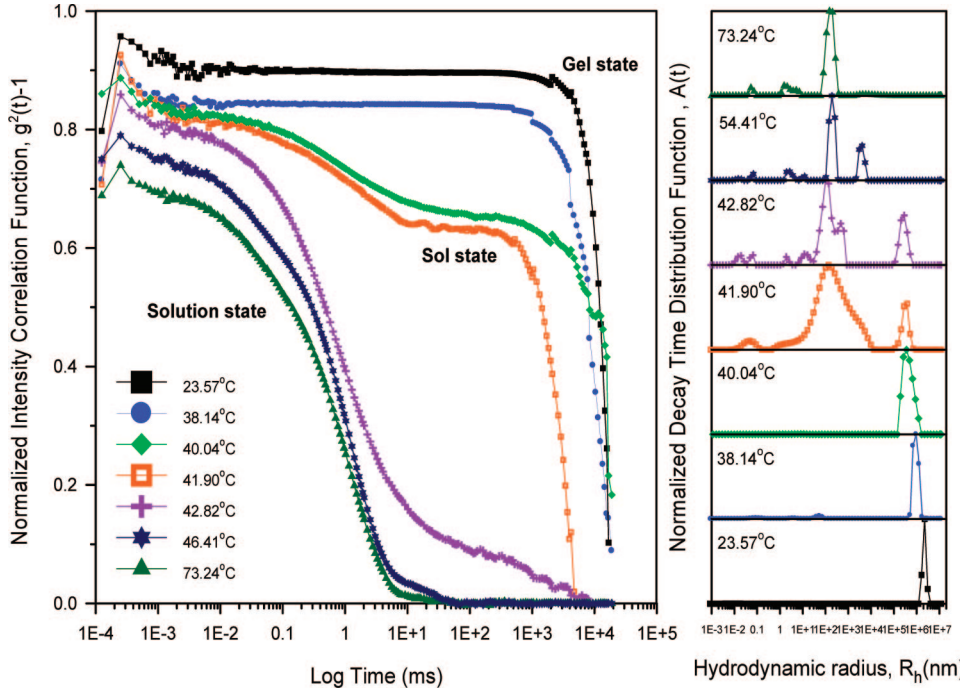

Figure 10. Normalized intensity correlation function, $g^2(t) - 1$, and the hydrodynamic radius (R_h) distribution of 1 wt % PF8/toluene gel measured in the heating cycle with a heating rate of 0.5 °C/min. Below ca. 40 °C where the system is apparently in the gel state, the decay of the correlation function occurs at very long time, and the corresponding R_h spectrum displays only the slowest mode with very larger size. As the gel-to-sol transition is approached, the correlation function profile changes markedly and the slowest mode in the R_h spectrum diminishes upon heating accompanied by growths of the slow mode, the intermediate mode, and the fast mode.

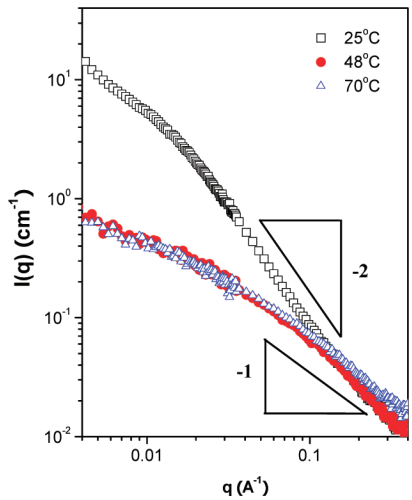

Figure 11. Temperature-dependent SANS profile of 3 wt % PF8/toluene gel. The power-law dependence of the SANS intensity changes from the q^{-2} to q^{-1} when the gel is heated to 48 °C, showing that the sheetlike aggregates melts and the rodlike PF8 chains forming the aggregates are redissolved into the solvent.

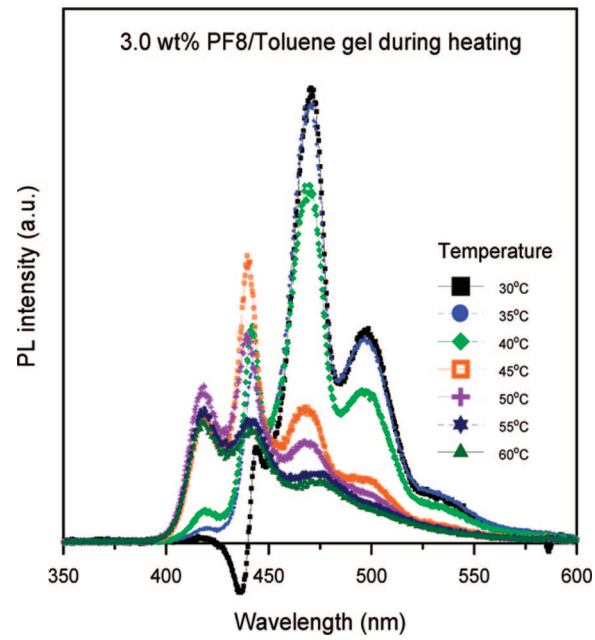

Figure 12. Temperature-dependent PL spectra of 3 wt % PF8/toluene gel. It can be seen that the emission intensities at 470 and 490 nm decrease while those at 420 and 448 nm increase progressively as the temperature is increased. The drop of the intensities of the peaks at 470 and 490 nm is the most drastic when the temperature is raised from 40 to 45 °C (i.e., across the gel-to-sol transition temperature).

The normalized intensity correlation function and the R_h distribution of 1.0 wt % PF8/toluene gel measured in the heating cycle are displayed in Figure 10. Below ca. 40 °C where the system was apparently in the gel state, the decay of the correlation function occurred at very long time, and the corresponding R_h spectrum displayed only the slowest mode with very larger size. As the gel-to-sol transition was approached, the correlation function profile changed markedly, and the slowest mode in the R_h spectrum diminished upon heating accompanied by growths of the slow mode, the intermediate mode, and the fast mode. The spectrum similar to that of the freshly prepared solution (Figure 2) was recovered at 73.2 °C, showing that the system attained the original solution structure (namely, coexistence of well-dissolved chains and network aggregates) at this temperature.

The gel-to-sol transition observed here had a direct relevance with the membrane-isotropic transition temperature (T^*_{mem}) defined by Knaapila et al.[31] This was manifested by the dissipation of the sheetlike aggregates or membranes within the

PF8-enriched phase across the gel-to-sol transition, as shown by the temperature-dependent SANS profile of 3 wt % PF8/toluene gel in Figure 11. The power-law dependence of the SANS intensity changed from the q^{-2} to q^{-1} when the gel was heated to 48 °C, showing that the sheetlike aggregates melted and the rodlike PF8 chains forming the aggregates were redissolved into the solvent.

The influence of the thermally induced gel-to-sol transition on the photoemission behavior was evaluated from the temperature-dependent PL experiment, where the PL spectrum was collected in situ in a heating cycle with the heating rate of 1.0 °C/min. Figure 12 shows the temperature-dependent PL spectra of 3 wt % PF8/toluene gel. It can be seen that the emission intensities at 470 and 490 nm decreased while those at 420 and 448 nm increased progressively as the temperature was increased, even before the gel-to-sol transition temperature was reached. This implied that the melting of the β-phase took place before the integrity of the sheetlike aggregates or the gel as a whole was disrupted. However, the drop of the intensities of the peaks at 470 and 490 nm was the most drastic when the temperature was raised from 40 to 45 °C (i.e., across the gel-to-sol transition temperature). The temperature-dependent PL spectra henced revealed that the heating across the gel-to-sol transition temperature (or T^*_{mem}) caused the dissociation of the sheetlike aggregates accompanied by the dissipation of the β-phase embedded within these aggregates.

Conclusions

In this work, we have provided insights into the gel formation of PF8/toluene semidilute solutions induced by cooling to subambient temperatures followed by prolonged aging. As the background information, the PF8 wormlike chains in the dilute toluene solution were found to extend significantly upon heating from 25 to 50 °C due to enhanced polymer−solvent attraction. Moreover, the polymer was found to form network aggregates in the semidilute solutions, which gave rise to a slow mode in the R_h spectrum. The gelation of PF8/toluene semidilute solution was driven by a macrophase separation at the subambient temperatures. In the course of the phase separation, the regions enriched with PF8 gradually developed the sheetlike aggregates in which a fraction of the chains or segments adopted the β-phase conformation. The presence of these sheetlike aggregates effectively immobilized the PF8-enriched domains, thereby preventing the system from attaining the equilibrium phase-separated morphology by the coarsening process. As a result, the phase-separated structure with extensive connectivity of the PF8-rich domains was dynamically arrested, and the system attainted the gel property. The β-phase dominated the photoluminescence spectrum of the gel, and the microstructure appeared to be effectively transferred into the film upon solvent removal as the PL spectrum of the cast film was essentially the same as that of the gel. The PF/toluene gel could be disintegrated by moderate heating. The gel-to-sol transition was accompanied by the disruptions of the sheetlike aggregates and the β-phase. The gel-to-sol hence resulted in a blue shift in the photoemission.

Acknowledgment. We acknowledge the financial support of the National Science Council of the Republic of China under Grants NSC 96-2221-E-168-007 and NSC 97-2752-E-002-PAE. The support of NIST, U.S. Department of Commerce, and the National Science Foundation, through Agreement No. DMR-9986442, in providing the neutron research facilities used in this work is gratefully acknowledged.

References and Notes

(1) (a) Burroughes, J. H.; Bradley, D. D. C.; Brown, A. R.; Marks, R. N.; Mackay, K.; Friend, R. H.; Burns, P. L.; Holmes, A. B. *Nature (London)* **1990**, *347*, 539–541. (b) Gross, M.; Müller, D. C.; Nothofer, H.-G.; Scherf, U.; Neher, D.; Bräuchle, C.; Meerholz, K. *Nature (London)* **2000**, *405*, 661–665.
(2) Hoppe, H.; Sariciftci, N. S. *J. Mater. Res.* **2004**, *19*, 1924–1945.
(3) Knaapila, M.; Stepanyan, R.; Lyons, B. P.; Torkkeli, M.; Monkman, A. P. *Adv. Funct. Mater.* **2006**, *16*, 599–609.
(4) Hoeben, F. J. M.; Jonkheijm, P.; Meijer, E. W.; Schenning, A. P. H. J. *Chem. Rev.* **2005**, *105*, 1491–1546.
(5) Neher, D. *Macromol. Rapid Commun.* **2001**, *22*, 1365–1385.
(6) Akcelrud, L. *Prog. Polym. Sci.* **2003**, *28*, 875–962.
(7) Cadby, J.; Lane, P. A.; Mellor, H.; Martin, S. J.; Grell, M.; Giebeler, C.; Bradley, D. D. C. *Phys. Rev. B* **2000**, *62*, 15604–15609.
(8) Grell, M.; Bradley, D. D. C.; Long, X.; Chamberlain, T.; Inbasekaran, M.; Woo, E. P.; Soliman, M. *Acta Polym.* **1998**, *79*, 439–444.
(9) Grell, M.; Bradley, D. D. C.; Ungar, G.; Hill, J.; Whitehead, K. S. *Macromolecules* **1999**, *32*, 5810–5817.
(10) Ariu, M.; Lidzey, D. G.; Bradley, D. D. C. *Synth. Met.* **2000**, *111*−*112*, 607–610.
(11) Kawana, S.; Durrell, M.; Lu, J.; MacDonald, J. E.; Grell, M.; Bradley, D. D. C.; Jukes, P. C.; Jones, R. A. L.; Bennett, S. L. *Polymer* **2002**, *43*, 1907–1913.
(12) Winokur, M. J.; Slinker, J.; Huber, D. L. *Phys. Rev. B* **2003**, *67*, 184106.
(13) Misaki, M.; Ueda, Y.; Nagamatsu, S.; Yoshida, Y.; Tanigaki, N.; Yase, K. *Macromolecules* **2004**, *37*, 6926–6931.
(14) Rothe, C.; King, S. M.; Dias, F.; Monkman, A. P. *Phys. Rev. B* **2004**, *70*, 195213.
(15) Chen, S. H.; Chou, H. L.; Su, A. C.; Chen, S. A. *Macromolecules* **2004**, *37*, 6833–6838.
(16) Chen, S. H.; Su, A. C.; Chen, S. A. *J. Phys. Chem. B* **2005**, *109*, 10067–10072.
(17) Chen, S. H.; Su, A. C.; Su, C. H.; Chen, S. A. *Macromolecules* **2005**, *38*, 379–385.
(18) Chunwaschirasiri, W.; Tanto, B.; Huber, D. L.; Winokur, M. J. *Phys. Rev. Lett.* **2005**, *94*, 107402. (1−4).
(19) Arif, M.; Volz, C.; Guha, S. *Phys. Rev. Lett.* **2006**, *96*, 025503.
(20) Knaapila, M.; Garamus, V. M.; Dias, F. B.; Almásy, L.; Galbrecht, F.; Charas, A.; Morgado, J.; Burrows, H. D.; Scherf, U.; Monkman, A. P. *Macromolecules* **2006**, *39*, 6505–6512.
(21) Campoy-Quiles, M.; Sims, M.; Etchegoin, P. G.; Bradley, D. D. C. *Macromolecules* **2006**, *39*, 7673–7680.
(22) Chen, S.; Su, A. C.; Chen, S. A. *Macromolecules* **2006**, *39*, 9143–9149.
(23) Bradley, D. D. C.; Grell, M.; Grice, A.; Tajbakhsh, A. R.; O'Brien, D. F.; Bleyer, A. *Opt. Mater.* **1998**, *9*, 1–11.
(24) Grell, M.; Bradley, D. D. C.; Inbasekaran, M.; Woo, E. P. *Adv. Mater.* **1997**, *9*, 798–802.
(25) (a) Banach, M. J.; Friend, R. H.; Sirringhaus, H. *Macromolecules* **2004**, *37*, 6079–6085. (b) Nguyen, T.-Q.; Doan, V.; Schwartz, B. J. *J. Chem. Phys.* **1999**, *110*, 4068–4078.
(26) Chen, S. H.; Su, A. C.; Chang, C. S.; Chen, H. L.; Ho, D. L.; Tsao, C. S.; Peng, K. Y.; Chen, S. A. *Langmuir* **2004**, *20*, 8909–8915.
(27) Li, Y. C.; Chen, K. B.; Chen, H. L.; Hsu, C. S.; Tsao, C. S.; Chen, J. H.; Chen, S. A. *Langmuir* **2006**, *22*, 11009–11015.
(28) Rahman, M. H.; Chen, C. Y.; Liao, S. C.; Chen, H. L.; Tsao, C. S.; Chen, J. H.; Liao, J. L.; Ivanov, V. A.; Chen, S. A. *Macromolecules* **2007**, *40*, 6572–6578.
(29) Knaapila, M.; Dias, F. B.; Garamus, V. M.; Almasy, L.; Torkkeli, M.; Leppanen, K.; Galbrecht, F.; Preis, E.; Burrows, H. D.; Scherf, U.; Monkman, A. P. *Macromolecules* **2007**, *40*, 9398–9405.
(30) Perahia, D.; Traiphol, R.; Bunz, U. H. F. *J. Chem. Phys.* **2002**, *117*, 1827–1832.
(31) Knaapila, M.; Stepanyan, R.; Torkkeli, M.; Garamus, V. M.; Galbrecht, F.; Nehls, B. S.; Preis, E.; Scherf, U.; Monkman, A. P. *Phys. Rev. E* **2008**, *77*, 051803.
(32) (a) Zimm, B. H. *J. Chem. Phys.* **1948**, *16*, 1093–1098. (b) Zimm, B. H. *J. Chem. Phys.* **1948**, *16*, 1099–1116.
(33) Fang, L.; Brown, W.; Koňák, Č. *Macromolecules* **1991**, *24*, 6839–6842.
(34) Martin, J. E.; Wilcoxon, J. P. *Phys. Rev. Lett.* **1988**, *61*, 373–376.
(35) Adam, M.; Delsanti, M.; Munch, J. P.; Durand, D. *Phys. Rev. Lett.* **1988**, *61*, 706–709.
(36) Ren, S. Z.; Shi, W. F.; Zhang, W. B.; Sorensen, C. M. *Phys. Rev. A* **1992**, *45*, 2416–2422.
(37) Schmitz, K. S. *An Introduction to Dynamic Light Scattering by Macromolecules*; Academic Press: New York, 1990.
(38) Brown, W. *Dynamic Light Scattering*; Clarendon Press: Oxford, 1993.

(39) Fytas, G.; Nothofer, H. G.; Scherf, U.; Vlassopoulos, D.; Meier, G. *Macromolecules* **2002**, *35*, 481–488.
(40) Perahia, D.; Jiao, X.; Traiphol, R. *J. Polym. Sci., Part B* **2004**, *42*, 3165–3178.
(41) (a) Gettinger, C. L.; Heeger, A. J.; Drake, J. M.; Pine, D. J. *J. Chem. Phys.* **1994**, *101*, 1673–1678. (b) Kratky, O.; Porod, G. *Recl. Trav. Chim. Pays-Bas* **1949**, *68*, 1106–1122.
(42) Amis, E. J.; Janmey, P. A.; Ferry, J. D.; Yu, H. *Macromolecules* **1983**, *16*, 441–446.
(43) Teraoka, I. *Polymer Solutions: An Introduction to Physical Properties*; John Wiley & Sons: New York, 2002.
(44) Kromer, H.; Kuhn, R.; Pielartzik, H.; Siebke, W.; Eckhardt, V.; Schmidt, M. *Macromolecules* **1991**, *24*, 1950–1954.
(45) Khan, A. L. T.; Banach, M. J.; Kohler, A. *Synth. Met.* **2003**, *139*, 905–907.
(46) Zhu, R.; Lin, J. M.; Wang, W. Z.; Zheng, C.; Wei, W.; Huang, W.; Xu, Y. H.; Peng, J. B.; Cao, Y. *J. Phys. Chem. B* **2008**, *112*, 1611–1618.
(47) Neher, D. *Macromol. Rapid Commun.* **2001**, *22*, 1365–1385.
(48) Traiphol, R.; Charoenthai, N. *Synth. Met.* **2008**, *158*, 135–142.
(49) Barbara, P. F.; Gesquiere, A. J.; Park, S. J.; Lee, Y. J. *Acc. Chem. Res.* **2005**, *38*, 602–610.
(50) Hennebicq, E.; Deleener, C.; Brédas, J.-L.; Scholes, G. D.; Beljonne, D. *J. Chem. Phys.* **2006**, *125*, 054901.

MA802408U